AFRL-RZ-WP-TP-2010-2091

CONTROL OF $BaZrO_3$ NANOROD ALIGNMENT IN $YBa_2Cu_3O_{7-x}$ THIN FILMS BY MICROSTRUCTURAL MODULATION (POSTPRINT)

F.J. Baca, R.L.S. Emergo, and J.Z. Wu

University of Kansas

Paul N. Barnes, Timothy J. Haugan, and J.N. Reichart

Mechanical Energy Conversion Branch
Energy/Power/Thermal Division

MARCH 2010

AIR FORCE RESEARCH LABORATORY
PROPULSION DIRECTORATE
WRIGHT-PATTERSON AIR FORCE BASE, OH 45433-7251
AIR FORCE MATERIEL COMMAND
UNITED STATES AIR FORCE

REPORT DOCUMENTATION PAGE

Form Approved
OMB No. 0704-0188

1. REPORT DATE *(DD-MM-YY)*	2. REPORT TYPE	3. DATES COVERED *(From - To)*
March 2010	Journal Article Postprint	01 August 2005 – 01 August 2008

4. TITLE AND SUBTITLE

CONTROL OF $BaZrO_3$ NANOROD ALIGNMENT IN $YBa_2Cu_3O_{7-x}$ THIN FILMS BY MICROSTRUCTURAL MODULATION (POSTPRINT)

5a. CONTRACT NUMBER
In-house

5b. GRANT NUMBER

5c. PROGRAM ELEMENT NUMBER
62203F

6. AUTHOR(S)

F.J. Baca, R.L.S. Emergo, and J.Z. Wu (University of Kansas)
Paul N. Barnes, Timothy J. Haugan, and J.N. Reichart (AFRL/RZPG)

5d. PROJECT NUMBER
3145

5e. TASK NUMBER
32

5f. WORK UNIT NUMBER
314532ZE

7. PERFORMING ORGANIZATION NAME(S) AND ADDRESS(ES)

University of Kansas
Department of Physics and Astronomy
Lawrence, KS 66045

Mechanical Energy Conversion Branch (AFRL/RZPG)
Energy/Power/Thermal Division
Air Force Research Laboratory, Propulsion Directorate
Wright-Patterson Air Force Base, OH 45433-7251
Air Force Materiel Command, United States Air Force

8. PERFORMING ORGANIZATION REPORT NUMBER
AFRL-RZ-WP-TP-2010-2091

9. SPONSORING/MONITORING AGENCY NAME(S) AND ADDRESS(ES)

Air Force Research Laboratory
Propulsion Directorate
Wright-Patterson Air Force Base, OH 45433-7251
Air Force Materiel Command
United States Air Force

10. SPONSORING/MONITORING AGENCY ACRONYM(S)
AFRL/RZPG

11. SPONSORING/MONITORING AGENCY REPORT NUMBER(S)
AFRL-RZ-WP-TP-2010-2091

12. DISTRIBUTION/AVAILABILITY STATEMENT

Approved for public release; distribution unlimited.

13. SUPPLEMENTARY NOTES

Journal article published in the *Applied Physics Letters,* Vol. 94 (2009). The journal article contains color.
PA Case Number: 88ABW-2008-1171; Clearance Date: 02 Dec 2008.

14. ABSTRACT

The alignment of $BaZrO_3$-nanorods (BZO-NR) in $YBa_2Cu_3O_{7-x}$ was studied using vicinal substrates to modulate the microstructure. As the vicinal angle was increased to 10°, the angular splay of BZO-NRs increased. Correspondingly, the vortex pinning along the *c*-axis increased slightly, a possible consequence of enhanced vortex entanglement. Up to 10°, an increasing density of planar defects was observed, while at ~20° an orthogonal reorientation of the BZO-NRs along the *a*-*b* planes occurs. This suggests that the modulated microstructure introduces a competing effect on the BZO-NR formation and alignment, and beyond a critical vicinal angle, *c*-axis alignment is no longer favorable for BZO-NRs.

15. SUBJECT TERMS

superconductivity, flux pinning, critical current density, magnetic field, $YBa_2Cu_3O_{7-z}$ or YBCO, nanorods, vicinal substrates

16. SECURITY CLASSIFICATION OF:			17. LIMITATION OF ABSTRACT:	18. NUMBER OF PAGES	19a. NAME OF RESPONSIBLE PERSON (Monitor)
a. REPORT	b. ABSTRACT	c. THIS PAGE			Timothy J. Haugan
Unclassified	Unclassified	Unclassified	SAR	10	19b. TELEPHONE NUMBER *(Include Area Code)* N/A

Standard Form 298 (Rev. 8-98)
Prescribed by ANSI Std. Z39-18

Control of $BaZrO_3$ nanorod alignment in $YBa_2Cu_3O_{7-x}$ thin films by microstructural modulation

F. J. Baca,[1,2,a)] P. N. Barnes,[1] R. L. S. Emergo,[2] T. J. Haugan,[1] J. N. Reichart,[1] and J. Z. Wu[2]
[1]*U. S. Air Force Research Laboratory, Propulsion Directorate, WPAFB, Ohio 45433, USA*
[2]*Department of Physics and Astronomy, University of Kansas, Lawrence, Kansas 66045, USA*

(Received 5 December 2008; accepted 11 February 2009; published online 11 March 2009)

The alignment of $BaZrO_3$-nanorods (BZO-NRs) in $YBa_2Cu_3O_{7-x}$ was studied using vicinal substrates to modulate the microstructure. As the vicinal angle was increased to 10°, the angular splay of BZO-NRs increased. Correspondingly, the vortex pinning along the *c*-axis increased slightly, a possible consequence of enhanced vortex entanglement. Up to 10°, an increasing density of planar defects was observed, while at ~20° an orthogonal reorientation of the BZO-NRs along the *a*-*b* planes occurs. This suggests that the modulated microstructure introduces a competing effect on the BZO-NR formation and alignment, and beyond a critical vicinal angle, *c*-axis alignment is no longer favorable for BZO-NRs. © *2009 American Institute of Physics*. [DOI: 10.1063/1.3097234]

Microstructure engineering provides an effective way to improve the magnetic vortex pinning via insertion of nanoscale objects into the superconductor matrix. Precise control of these nano-objects, including their dimension and alignment, is critical to obtaining optimal pinning effects and the increased in-field critical current density $J_c(H)$ necessary for many applications. In $YBa_2Cu_3O_{7-x}$ (YBCO) thin films, insertion of these defects has been accomplished by the addition of nanoimpurities of materials such as Y_2BaCuO_5, $BaZrO_3$ (BZO), and $BaSnO_3$ (BSO) or the introduction of structural defects via ion irradiation and substrate surface decoration.[1–8] Notably, BZO and BSO form self-assembled nanorods (NRs) that align nearly along the direction of the YBCO *c*-axis, a feature of particular interest as they serve to improve the vortex pinning for magnetic fields applied in this direction.[3,4]

While extended columnar defects provide an increased overall pinning force as they effectively pin the vortices along their length, it was shown that a splay of defect alignments reduces the likelihood of vortex hopping by virtue of the column configuration. This defect geometry results in greater pinning at increased magnetic fields when compared to columns more uniformly aligned with the *c*-axis.[9–12] This then suggests that the control of the defect alignment is beneficial for improving both the angular anisotropy of J_c and the overall vortex pinning.

Therefore, to achieve the controlled alignment of the defects, such as BZO-NRs, we seek structural parameters that may be tuned to produce these desired results. Parameters such as microstructural strain and the alignment of dislocations are considered to be important in the formation of BZO-NRs in YBCO.[3,13–15] Therefore, since a vicinal surface provides a means to modulate the microstructural properties, we have examined the effects induced in BZO-doped YBCO thin films deposited on miscut $SrTiO_3$ substrates. Our experiments presented here show that with increasing vicinal angle, significant changes in the microstructure and $J_c(H,\theta)$ behaviors are observable. At smaller vicinal angles of up to 10°, the BZO columns become splayed, while at higher angles, a significant change in the direction of alignment of the BZO-NRs within the YBCO matrix occurs, showing that the substrate-level surface modulation indeed provides a mechanism to change the direction of alignment of the BZO columns.

YBCO films with 2 vol % BZO were deposited via single-target pulsed laser deposition using a KrF laser ($\lambda = 248$ nm) at an 8 Hz repetition rate. The substrates were held at 800 °C during the deposition, with an O_2 partial pressure of 300 mTorr. Films approximately 200 nm thick were grown on STO substrates with miscut angles of 0°, 5°, 10°, and 20°. The samples were patterned by photolithography, and transport properties were measured in the direction parallel to the vicinal steps via a four-point probe.[16] To study the microstructural properties by transmission electron microscopy (TEM), cross sections were prepared using FEI Nova 600 NanoLab and DB235 focused ion beam systems. Care was taken to cut the cross-sectional foils perpendicular to the vicinal steps so that the effects of the modulated surface could be directly observed. The microstructures of the films were studied using a Philips CM200 and FEI Titan TEM operating at 200 and 300 kV, respectively.

The cross-sectional TEM images in Fig. 1 illustrate the microstructures of the vicinal films for miscut angles of 0°, 5°, 10°, and 20°. For comparison, Fig. 1(a) shows a nonvicinal BZO-doped YBCO film with NRs 5–6 nm in diameter, as commonly observed. The 5° vicinal sample in Fig. 1(b) shows only slight microstructural change when compared to the nonvicinal film, and higher resolution images show that the YBCO *a*-*b* planes form roughly parallel to the vicinal terraces. The BZO-NRs show a slight misalignment of approximately $9.7 \pm 3.1°$ from the tilted *c*-axis, which happens to be a comparable splay to that reported by Civale *et al.*[10] for high energy Sn irradiated YBCO. For comparison, the nonvicinal BZO-NRs show a misalignment angle of $5.3 \pm 2.4°$. Therefore, from the increased columnar splay in the vicinal film, we may expect increased vortex entanglement and corresponding increase in the in-field J_c.

The highly defective YBCO microstructure of the 10° sample, with a significant occurrence of stacking faults, is shown in Fig. 1(c). These types of structural defects have

a)Electronic mail: francisco.baca@wpafb.af.mil, jbaca@ku.edu.

0003-6951/2009/94(10)/102512/3/$25.00

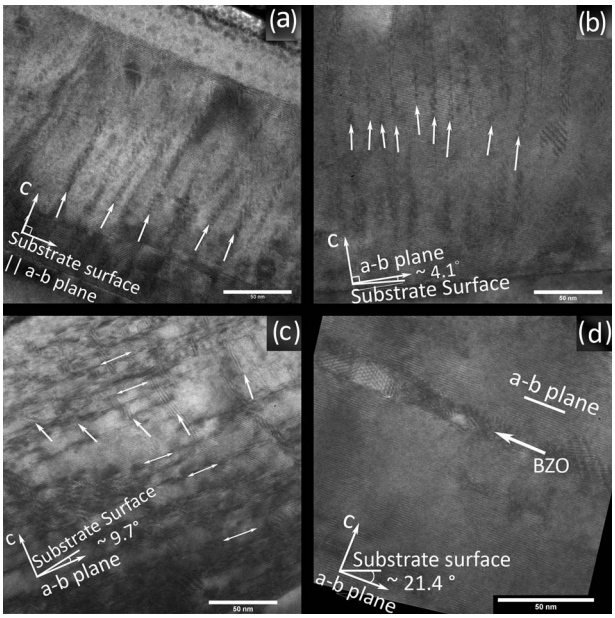

FIG. 1. Bright field cross-sectional TEM images of 2 vol % BZO-doped YBCO films. The single ended arrows point to examples of BZO-NRs, and the scale bars indicate 50 nm. (a) Nonvicinal film showing typical *c*-axis alignment. (b) 5° vicinal with 9.7° ± 3.1° NR splay. (c) Highly defective YBCO lattice of 10° vicinal film. The double-sided arrows show examples of planar defects. (d) 20° vicinal showing BZN-NR aligned with *a*-*b* planes.

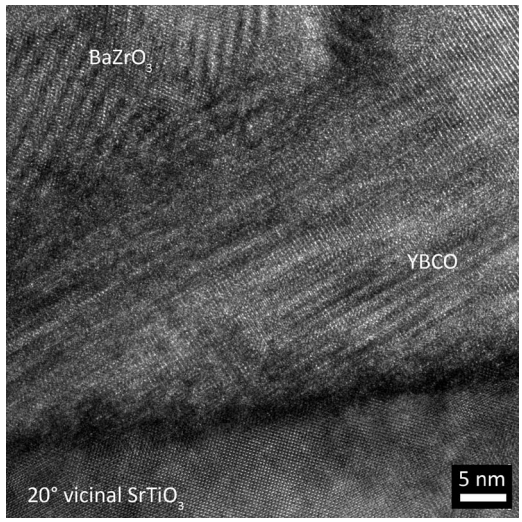

FIG. 2. High-resolution TEM image of 20° vicinal YBCO with 2 vol % BZO showing the edge of a BZO-NR aligned with the YBCO *a*-*b* planes. The scale bar indicates 5 nm.

been reported for pure YBCO growth on vicinal substrates.[17] However, the high density of stacking faults observed here shows that the effect appears to be exaggerated perhaps by the additional elastic strain on the YBCO matrix induced by the BZO-NRs and the approximately 9% lattice mismatch between them. Additionally, the continuity of the BZO-NRs through the film thickness is reduced, implying that the $H \| c$ pinning may be slightly diminished by the reduction in total pinning force.

The most drastic microstructural change, however, is observed in the 20° vicinal film shown in Fig. 1(d). At this miscut angle, the BZO-NR alignment is rotated roughly 90° such that its axis is oriented nearly parallel to the YBCO *a*-*b* planes. In addition, the diameter of the BZO-NRs is increased to approximately 10.8 ± 1.5 nm, nearly twice the diameter of those in the nonvicinal films. Figure 2 shows a higher resolution image of a BZO-NR on a 20° miscut STO substrate. It is also notable that as the vicinal angle is increased from 10° to 20°, the density of stacking faults diminishes significantly. The reorientation of the BZO-NR with increased miscut angle suggests that the microstructural conditions that dictate their direction of alignment are strongly linked to parameters influenced by vicinal growth. These parameters including strain and dislocation alignment are suggested to play a significant role in the self-assembly of NRs within the YBCO matrix in nonvicinal films.[3,13–15] However, the surface modulation of the vicinal steps clearly incorporates additional degrees of complexity to the strain relationships between the BZO-NRs and the YBCO matrix. For example, given an interface between materials of differing lattice constants a_1 and a_2, the dislocation spacing D is predicted to follow the relationship $D = a_{avg}^2 / |a_1 - a_2|$.[18] If we approximate the orthorhombic YBCO unit cell as a trilayered cubic, then for a nonvicinal YBCO/BZO interface, the average dislocation spacing would be approximately 5–6 nm.[13,17] However, we previously reported dislocations spaced by roughly 14 nm in 10° vicinal BZO-doped films.[19] This suggests a possible correlation between the vicinal angle and the spacing of the dislocations that drive the assembly of the BZO-NRs and can potentially account for the increasingly misaligned rods from the *c*-axis.

It was suggested by Haage, *et al.*[17] that when a vicinal step is not of a specific height (matching with one block of the layered unit cell), the formation of an antiphase boundary occurs accompanied by a stacking fault. Therefore the occurrence of dislocations is expected in vicinal films of pure YBCO, from which the long-range effects may be expected to influence the dislocation density of the second-phase inclusions. It is then possible that by increasing the vicinal angle beyond a critical value, the occurrence of dislocations may become more favorable within the YBCO *a*-*b* planes as opposed to along the *c*-axis. This is supported by the relative lack of stacking faults observed in the 20° vicinal sample and by the rotated direction of BZO-NR alignment in these films.

The values listed in Table I show that the superconducting transition temperatures (T_c) of the vicinal films, ~90.1–92.1 K, were not depressed by the addition of the BZO to the same extent as their nonvicinal counterpart (T_c ~89.0 K). Measurements by x-ray diffraction have shown a decrease in the *c*-axis length of BZO-doped YBCO when grown on vicinal substrates. From this, the reduced spacing between Cu–O planes was suggested to lead to a smaller decrease in T_c.[20] The slightly lower T_c of the 20° sample may also indicate an overall reduction in microstructural strain

TABLE I. Superconducting transition temperatures (onset, determined magnetically) T_c and self-field critical current densities J_c (77 K, along longitudinal direction) for vicinal angles from 0° to 20°.

Vicinal angle (°)	T_c (K)	J_c (SF, 77 K) (MA/cm^2)
0	89.0	2.7
5	90.1	5.4
10	92.1	6.4
20	91.1	5.4

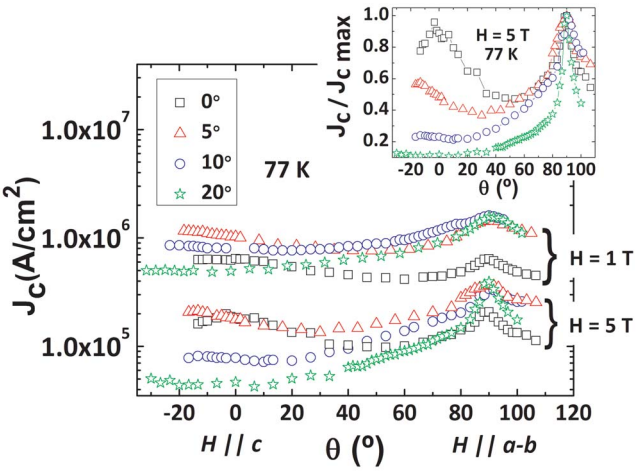

FIG. 3. (Color online) Angular dependence of the transport critical current density (J_c) for 0°–20° vicinal films at 77 K for applied magnetic fields of 1 and 5 T. The inset shows J_c (77 K, 5 T) normalized to the maximum values $J_{c\,\max}$. For the sake of comparison at $H\|c$ and $H\|a$-b, the J_c curves have been shifted such that the $J_c(\theta=90°)$ peaks coincide.

due to the preferred state of the realigned BZO-NRs. The microstructural modifications also have a direct effect on the flux pinning properties of the films as evident in Fig. 3. $J_c(\theta)$ for 1 and 5 T fields at 77 K are shown in Fig. 3, while the inset shows $J_c(\theta)$ at 5 T normalized to their maximum values, $J_{c\,\max}$. Because the crystallographic axes of the vicinal samples are tilted with respect to the substrate normal, the measured angle used to determine $H\|a$-b is shifted. Therefore, the J_c plots have been shifted such that the $H\|a$-b peaks coincide at $\theta=90°$. The curves in Fig. 3 show that the 5° vicinal sample gives increased values of J_c for $H\|c$ at 1 T when compared to the nonvicinal film, while at 5 T these peaks are nearly equal. Thus the $H\|c$ pinning behavior of the splayed BZO-NRs in the vicinal film is consistent with that attributed to reduced vortex hopping in the splayed ion damage tracks in irradiated YBCO for applied magnetic fields less than the matching field.[10,11] This may indicate that analogous mechanisms of vortex entanglement are indeed responsible in a range of $H<5$ T. The reduced density and continuity of *c*-axis aligned defects are also evident in Fig. 3 for the 10° film where $J_c(H\|c)$ peak is reduced at 1 T and diminished at 5 T. As would be expected by the lack of correlated *c*-axis defects, the $J_c(\theta)$ dependence is nearly flat for $H\|c$ in the 20° sample. This exemplifies one extreme of an overall trend of decreasing *c*-axis defect correlation and increased *a*-*b* pinning with increasing miscut angle, as illustrated in the inset of Fig. 3. In this plot, the relative ratio of the *c*-axis peak to the *a*-*b*-axis peak, $J_c(\theta=0°)/J_c(\theta=90°)$, consistently decreases as the vicinal angle increases from 0° to 20° at 5 T. A parallel trend is followed at 1 T but with higher values, also indicating that the number of vortices exceeds the available pinning sites at 5 T. This suggests that an increased concentration of BZO-NRs may produce even greater vortex pinning for fields above 1 T.

In conclusion, an overall increase in $J_c(\theta)$ at 77 K in applied magnetic fields is shown for vicinal BZO-doped YBCO films up to a 10° miscut angle, while at 20°, improvements are seen for $H\|a$-b. The increased density of stacking faults and dislocations at vicinal angles up to 10° indicates a change in the microstructural evolution as the miscut angle is increased. This change is further exemplified on the 20° miscut substrates as the dislocation spacing is increased beyond a critical threshold and BZO-NR formation becomes favorable in the direction parallel to the YBCO *a*-*b* planes. Since the lattice mismatch between BSO and YBCO is smaller than that of BZO, additional studies on the effect of the vicinal angle on the dislocation spacing in both of these systems should allow us to better substantiate the mechanism of NR alignment in these strain-modulated films.

The authors acknowledge support from the Air Force Office of Scientific Research, the Air Force Research Laboratory, the National Science Foundation (DMR0803149), and the Department of Energy (DE-FG03–01ER45911).

[1]T. Haugan, P. N. Barnes, R. Wheeler, F. Meisenkothen, and M. Sumption, Nature (London) **430**, 867 (2004).
[2]J. L. MacManus-Driscoll, S. R. Foltyn, Q. X. Jia, H. Wang, A. Serquis, L. Civale, B. Maiorov, M. E. Hawley, M. P. Maley, and D. E. Peterson, Nature Mater. **3**, 439 (2004).
[3]A. Goyal, S. Kang, K. J. Leonard, P. M. Martin, A. A. Gapud, M. Varela, M. Paranthaman, A. O. Ijaduola, E. D. Specht, J. R. Thompson, D. K. Christen, S. J. Pennycook, and F. A. List, Supercond. Sci. Technol. **18**, 1533 (2005).
[4]C. V. Varanasi, P. N. Barnes, J. Burke, L. Brunke, I. Maartense, T. J. Haugan, E. A. Stinzianni, K. A. Dunn, and P. Haldar, Supercond. Sci. Technol. **19**, L37 (2006).
[5]L. Civale, Supercond. Sci. Technol. **10**, A11 (1997).
[6]T. Aytug, M. Paranthaman, K. J. Leonard, S. Kang, P. M. Martin, L. Heatherly, A. Goyal, A. O. Ijaduola, J. R. Thompson, D. K. Christen, R. Meng, I. Rusakova, and C. W. Chu, Phys. Rev. B **74**, 184505 (2006).
[7]P. Mele, K. Matsumoto, T. Horide, O. Miura, A. Ichinose, M. Mukaida, Y. Yoshida, and S. Horii, Supercond. Sci. Technol. **19**, 44 (2006).
[8]F. J. Baca, D. Fisher, R. L. S. Emergo, and J. Z. Wu, Supercond. Sci. Technol. **20**, 554 (2007).
[9]T. Hwa, P. Le Doussal, D. R. Nelson, and V. M. Vinokur, Phys. Rev. Lett. **71**, 3545 (1993).
[10]L. Civale, L. Krusin-Elbaum, J. R. Thompson, R. Wheeler, A. D. Marwick, M. A. Kirk, Y. R. Sun, F. Holtzberg, and C. Field, Phys. Rev. B **50**, 4102 (1994).
[11]L. Krusin-Elbaum, A. D. Warwick, R. Wheeler, C. Field, V. M. Vinokur, G. K. Leaf, and M. Palumbo, Phys. Rev. Lett. **76**, 2563 (1996).
[12]R. Wheeler, M. A. Kirk, A. D. Warwick, L. Civale, and F. H. Holtzberg, Appl. Phys. Lett. **63**, 1573 (1993).
[13]J. P. Rodriguez, P. N. Barnes, and C. V. Varanasi, Phys. Rev. B **78**, 052505 (2008).
[14]Y. F. Gao, J. Y. Meng, A. Goyal, and G. M. Stocks, JOM **60**, 54 (2008).
[15]P. Mele, K. Matsumoto, T. Horide, A. Ichinose, M. Mukaida, Y. Yoshida, S. Horii, and R. Kita, Supercond. Sci. Technol. **21**, 032002 (2008).
[16]R. L. S. Emergo, J. Z. Wu, T. J. Haugan, and P. N. Barnes, Appl. Phys. Lett. **87**, 232503 (2005).
[17]T. Haage, J. Zegenhagen, J. Q. Li, H.-U. Habermeier, M. Cardona, Ch. Jooss, R. Warthmann, A. Forkl, and H. Kronmuller, Phys. Rev. B **56**, 8404 (1997).
[18]J. M. Woodall, G. D. Pettit, T. N. Jackson, C. Lanza, K. L. Kavanagh, and J. W. Mayer, Phys. Rev. Lett. **51**, 1783 (1983).
[19]F. J. Baca, R. L. Emergo, J. Z. Wu, T. J. Haugan, J. N. Reichart, and P. N. Barnes, IEEE Trans. Appl. Supercond. (unpublished).
[20]R. L. S. Emergo, F. J. Baca, J. Z. Wu, T. J. Haugan, and P. N. Barnes (unpublished).